Cellular and Molecular Life Sciences (2023) 80:331
https://doi.org/10.1007/s00018-023-04996-1

ORIGINAL ARTICLE

Juvenile hormone regulates silk gene expression by m^{6}A RNA methylation

Shuaiqi Liu[1] · Huan Tian[1] · Yusong Xu[1] · Huabing Wang[1]

Received: 4 July 2023 / Revised: 21 September 2023 / Accepted: 1 October 2023 / Published online: 23 October 2023

Abstract

Juvenile hormone (JH) is an indispensable insect hormone that is critical in regulating insect development and physiology. N6-methyladenosine (m^{6}A) is the most abundant modification of RNA that regulates RNA fate in eukaryotic organisms. However, the relationship between m^{6}A and JH remains largely unknown. Here, we found that the application of a Juvenile hormone analog (JHA) extended the larval period of *Bombyx mori* and increased the weight and thickness of the cocoon. Interestingly, global transcriptional patterns revealed that m^{6}A-related genes are specifically regulated by JHA in the posterior silk gland (PSG) that synthesizes the major component of cocoon silk. By transcriptome and m^{6}A sequencing data conjointly, we discovered that JHA significantly regulated the m^{6}A modification in the PSG of *B. mori* and many m^{6}A-containing genes are related to nucleic acid binding, nucleus, and nucleobase-containing compound metabolism. Notably, 547 genes were significantly regulated by JHA at both the m^{6}A modification and expression levels, especially 16 silk-associated genes, including *sericin2*, *seroin1*, *Serine protease inhibitors 4* (*BmSPI4*), *Serine protease inhibitors 5* (*BmSPI5*), and *LIM domain-binding protein 2* (*Ldb*). Among them, 11 silk associated genes were significantly affected by *METTL3* knockdown, validating that these genes are targets of m^{6}A modification. Furthermore, we confirm that JHA directly regulates the expression of *BmSPI4* and *BmSPI5* through m^{6}A modification of CDS regions. These results demonstrate the essential role of m^{6}A methylation regulated by JH in PSG, and elucidate a novel mechanism by which JH affects silk gland development via m^{6}A methylation. This study uncovers that m^{6}A modification is a critical factor mediating the effect of JH in insects.

✉ Huabing Wang
wanghb@zju.edu.cn

[1] College of Animal Sciences, Zhejiang University, Hangzhou 310058, China

Graphical abstract

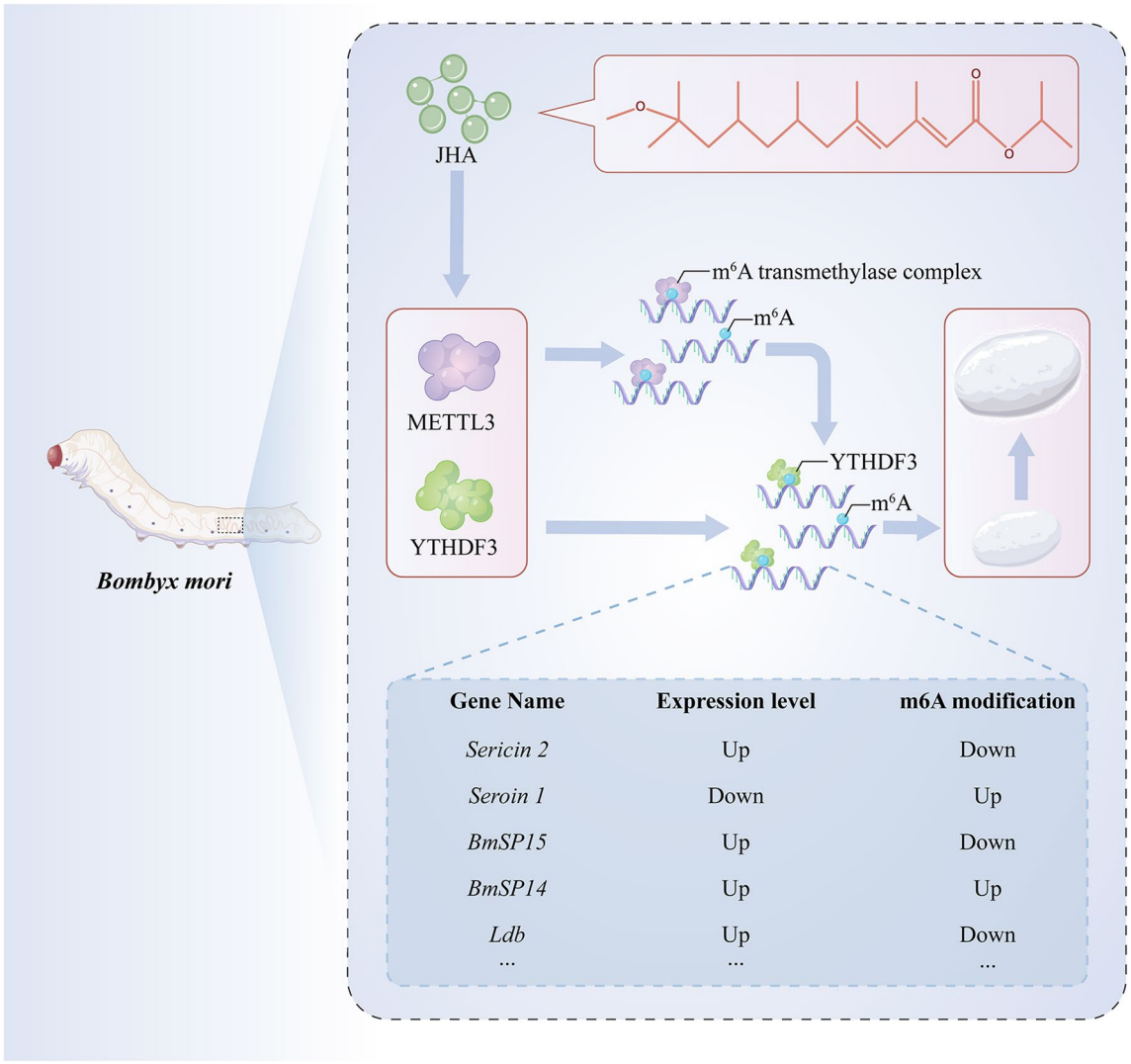

Keywords Insect · Juvenile hormone · m^{6}A · Silk gland · *Bombyx mori*

Introduction

Silk is a natural protein fiber known for its shine, strength, luster, and durability. In recent years, regenerated silk solutions were used to form a variety of biomaterials. Silk is usually made from cocoons that are spun by the silk gland of the domesticated silkworm, *Bombyx mori*. The increasing demand has driven notable efforts to improve silk production through hybrid breeding, but silk production has reached the long-expected plateau. The silk gland of *B. mori* is composed of three regions. The anterior silk gland is responsible for silk spinning, and the middle silk gland secretes sericin. The posterior silk gland synthesizes fibroin, the major component of cocoon silk. Juvenile hormone (JH) was used to improve the yield of silk in silk production. Juvenile hormone (JH) plays a crucial role in preserving larval characteristics and regulating various other biological processes in insects [1]. In *B. mori*, JH could induce the expression of *Bmdimm*, a transcription factor in the larval silk gland and contribute to the synthesis of fibroin H-chain protein [2–4]. JH restrains *BmTINP1*, which is involved in silk production, translocation from the nucleus to the cytoplasm [5]. The cross-talk of 20-hydroxyecdysone and JH regulates the transcription of *FMBP-1*, a novel transcription factor influencing

fib-H transcription [6]. The idea that stimulating fibroin protein synthesis by JHA treatment could improve silk yield is very attractive; however, little is known about the molecular mechanisms underlying the effect of JHA in the silkworm posterior silk gland on silk yield increase [7].

The regulation of JH is extensively involved in numerous aspects of insect life. Previous studies on JH in insects have mainly concentrated on JH directly regulating the transcription, translation, and translocation of specific genes [8–11]. For example, JH induced the expression of *Kruppel homolog 1*, thereby repressing the metamorphic differentiation of *Drosophila* adult abdominal epidermis [12]. Epigenetic studies on JH have become widespread and are gradually gaining attention. For example, the potential targets of CoREST, an integral component of chromatin corepressor complexes, are involved in the JH signaling pathway and lead to a switch to minor-like caste foraging behavior in *Camponotus floridanus* [13]. In *Tribolium castaneum*, deacetylation and acetylation of histones mediated by acetylation proteins play an important role in JH action [14]. CREB-binding protein, a transcriptional coregulator with histone acetyltransferase activity, mediates acetylation of H3K27 for JH induction of target genes in *T. castaneum* [15]. N6-methyladenosine modification is the most abundant and widespread internal modification found in the RNA of eukaryotic organisms. This modification plays a crucial role in maintaining the stability and effectiveness of mRNA during the process of translation [16–20]. The regulation and recognition of m^{6}A modification is a dynamic process that involves the concerted action of different proteins, including demethylases, methyltransferases, and m^{6}A binding proteins. These proteins work together to ensure that the m^{6}A modification is properly recognized and regulated within the RNA, allowing for the efficient translation of mRNA [21, 22]. The evolutionary relationship of m^{6}A-related genes, including *METTL3*, *METTL14*, *YTHDF3*, *YTHDC*, and *FL2D*, is relatively conserved in insects [23]. m^{6}A is involved in various biological processes of insects. For example, m^{6}A plays a critical role in sex determination and neuronal function in *Drosophila* [24, 25]. The m^{6}A site in the 5' UTR of a P450 gene, *CYP4C64*, leads to thiamethoxam resistance in *Bemisia tabaci* [26]. METTL3, the indispensable component of the m^{6}A demethylase complex, influences *Bombyx mori* nucleopolyhedrovirus infection, cell cycle progression, and chromosome alignment in BmN cells [27, 28]. In *Apis mellifera*, three genes in JH biosynthesis, *JHAMT*, *Vg*, and *CYP314A1*, have different m^{6}A methylation levels between workers and queens in different larval stages. Treatment with the SAH hydrolysis inhibitor DAA, which has been confirmed in peripheral cells to mainly affect RNA processing through inhibition of m^{6}A methylation, could alter the titer of JH in worker larvae [29]. The present study indicates the potential correlation between the JH signaling pathway and m^{6}A modification. However, whether and how JH influences m^{6}A modification in insects is still unclear. Considering the significant association of m^{6}A modification with growth and development, this study aimed to investigate the potential role of m^{6}A in the action of JH.

In this study, we investigated whether JH regulates silk gene expression levels through RNA m^{6}A methylation. To detect the effect of insect hormones on m^{6}A-related genes, we performed transcriptome sequencing of multiple silkworm tissues after JHA and 20E treatment. Interestingly, many m^{6}A-related genes were specifically regulated by JHA in silkworm PSGs. To further reveal the regulation of JH in numerous biological processes of silkworms through m^{6}A modification, we conducted m^{6}A methylation and RNA sequencing in the silkworm PSGs after JHA treatment. Furthermore, we knocked down *METTL3* and performed transcriptome profiling analysis to identify the mechanism by which m^{6}A modification mediates the regulatory effect of JH. Conjoint analysis of the transcriptome and m^{6}A sequencing reveal that JH regulates many silk-associated genes in the silkworm PSG via m^{6}A modification. Our findings provide new insights into the pivotal regulatory role of JH mediated by m^{6}A.

Results

JH enhances the weight and thickness of silkworm cocoon

To identify the function of JHA in improving silk protein production in silkworms, we performed individual experiments on silkworm larvae. After JHA treatment for 24 h, we found that the application of JHA significantly extended the fifth larval instar of silkworm. JHA treatment extended the *B. mori* fifth instar from 8 to 11 days (Fig.S1). We further measured the effect of JHA on the weight and thickness of the cocoon. The results showed that JHA enhanced the weight of silkworm cocoons, especially those of male silkworm (Fig. 1A). In addition, we found that JHA treatment significantly increased the thickness of silkworm cocoons, both in males and females (Fig. 1B–C). Taken together, these results showed that the application of JH extended the larval period, increased the weight and thickness of the cocoon, and further enhanced silk production in silkworms.

Characteristics of m^{6}A modification in the transcriptome of silkworm posterior silk gland

To investigate the characteristics of m^{6}A modification in the PSG of silkworm, we performed m^{6}A methylation sequencing to identify specific locations of m^{6}A sites in the mRNA

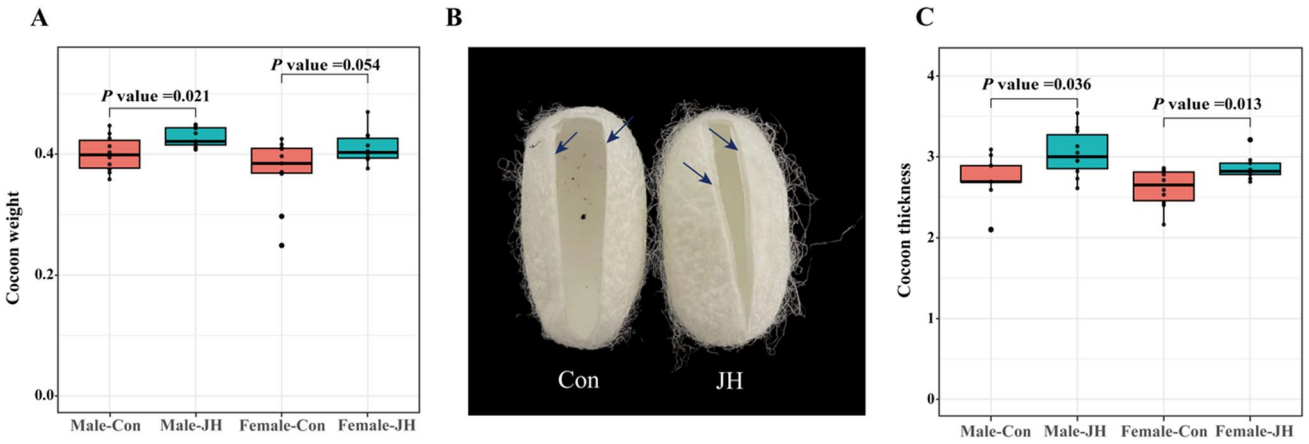

Fig. 1 JHA treatment enhanced the weight and thickness of silkworm cocoons. Comparison of cocoon weight between the control and JHA-treated groups (**A**). Comparison of cocoon thickness between the control and JHA-treated groups (**B** and **C**)

of PSG (Fig. 2A). Our results showed that m^{6}A modification was mainly enriched in exons and 3' UTRs, with particularly high levels of m^{6}A peaks observed around stop codons (Fig. 2B–C). Through the analysis of consensus motifs, we observed that the GGAC motif was enriched within m^{6}A sites (Fig. 2D). The motif has been frequently found in other studies on humans, mice, and fruit flies. To confirm the role of m^{6}A in the expression of genes, we further analyzed the relationship between the expression level, represented by FPKM, and the m^{6}A ratio of m^{6}A-containing genes. The results showed that the expression levels of m^{6}A-containing genes had a negative relationship with the m^{6}A modification

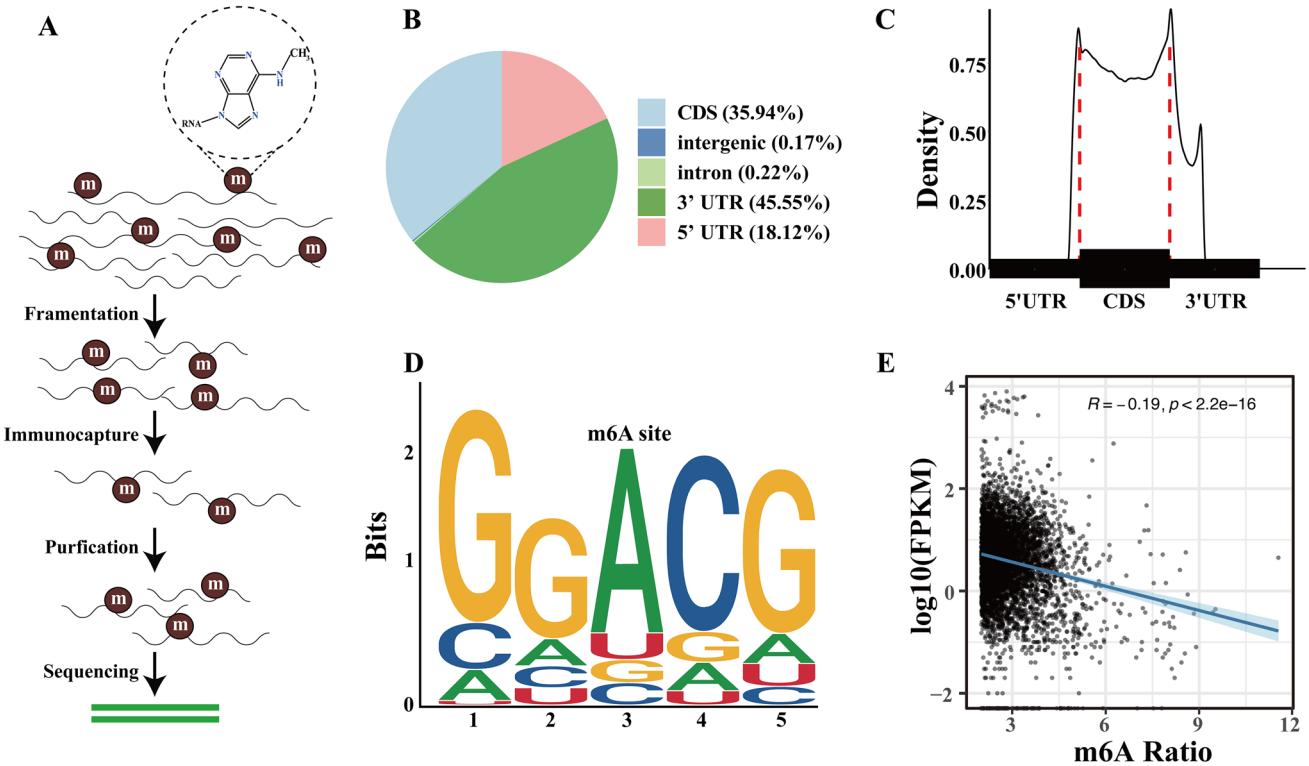

Fig. 2 Analysis of m^{6}A methylation sequencing in silkworm PSG: distribution, motif identification, and relationship with gene expression. Workflow of m^{6}A methylation sequencing, including RNA fragmentation, immunoprecipitation with a m^{6}A-specific antibody, mRNA purification, and sequencing (**A**). Pie chart showing the proportion of m^{6}A peaks in the indicated regions, such as CDS, 3' UTRs, and 5' UTRs (**B**). The profile of m^{6}A distribution across the transcriptome in silkworm PSG (**C**). The sequence motif of m^{6}A modification identified in silkworm PSG mRNA (**D**). Relationship between the gene m^{6}A modification ratio and expression levels (**E**)

levels of m^{6}A-containing genes (Fig. 2E). Collectively, the m^{6}A sequencing data provided clear evidence of the distribution features and consensus motifs of m^{6}A in the mRNA of silkworm PSG. These results suggested that m^{6}A modification in the mRNA of silkworm PSG tends to down-regulate gene expression.

m^{6}A-containing genes involved in several important biological pathways

m^{6}A modification is involved in various gene expression regulation and biological processes [30]. To investigate the role of m^{6}A in silkworm PSG, we performed Kyoto Encyclopedia of Genes and Genomes (KEGG) and Gene Ontology (GO) enrichment analysis on high-confidence m^{6}A-containing genes. From the m^{6}A-seq data, we identified 4962 high-confidence m^{6}A-containing genes. Seventy-four m^{6}A-containing genes are involved in the spliceosome and are critical for mRNA alternative splicing. Forty-four and 37 m^{6}A-containing genes were enriched in the mRNA surveillance pathway and RNA degradation, respectively (Fig. 3A). These pathways are important for the stability of mRNA. The results showed that m^{6}A-containing genes are involved in regulating the stability, splicing and translation of mRNA.

Furthermore, GO enrichment analysis revealed that 244 and 176 m^{6}A-containing genes were enriched in nucleic acid binding and nucleotide binding, respectively. Compared to molecular function terms, biological process terms, including gene expression, nucleic acid metabolic process, and RNA metabolic process, were enriched. Additionally, 277 m^{6}A-containing genes were enriched in the nucleus in the cellular component category (Fig. 3B). These results indicated that m^{6}A is closely related to nucleic acid binding and metabolic processes. Taken together, our findings suggest that m^{6}A plays a critical role in influencing RNA fate and regulating gene expression in the PSG of *B. mori*.

JH regulates the m^{6}A modification and expression level of genes in silkworm PSGs

To investigate the relationship between JH and m^{6}A modification, we performed transcriptome sequencing of multiple silkworm tissues after JHA treatment. Our findings indicated that the expression of m^{6}A-related genes was significantly changed by JHA treatment in PSG compared to other tissues (Fig.S2A). Western blotting also showed that JHA treatment significantly induced the protein expression of *METTL3* and *YTHDF3* in silkworm PSG (Fig.S2B). Additionally, we further found that JHA treatment significantly

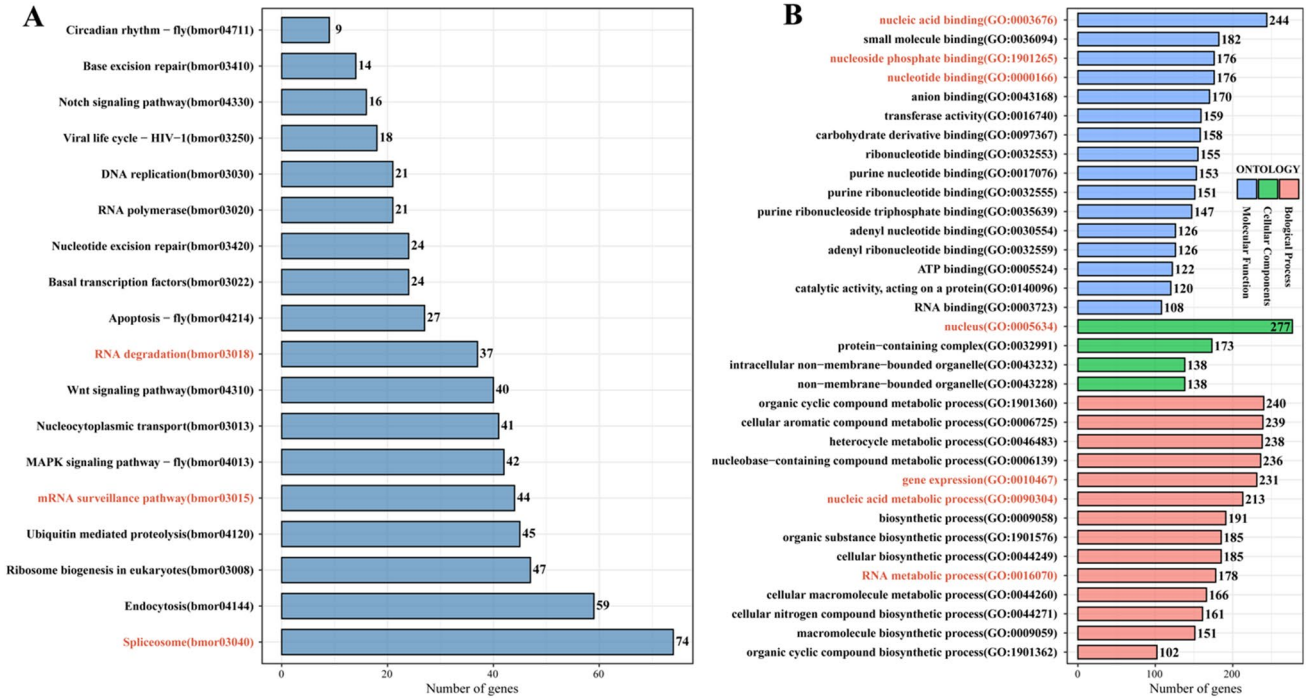

Fig. 3 KEGG and GO enrichment analysis of significant m^{6}A-containing genes identified in silkworm PSG m^{6}A-seq data. KEGG enrichment analysis of m^{6}A-containing genes identified in the m^{6}A-seq (**A**). GO enrichment analysis of biological process, cellular components, and molecular function for m^{6}A-containing genes identified in the m^{6}A-seq (**B**). Top 18 KEGG terms and GO terms containing more than 100 genes are listed to display the potential function of m^{6}A modification in silkworm PSG. Enriched GO and KEGG terms with $p < 0.05$ were represent in red color

increased the m^{6}A abundance of RNA in the PSG (Fig.S2C). The results indicated that JHA treatment affects the expression of *METTL3* and *YTHDF3*, thereby regulating the m^{6}A abundance of RNA in the PSG of silkworms.

We further performed m^{6}A sequencing of PSGs after JHA treatment. By analyzing transcriptome and m^{6}A sequencing data conjointly, we found 3795 differentially m^{6}A-modified genes (DMGs) and 3961 differentially expressed genes (DEGs) in m^{6}A-seq and RNA-seq of silkworm PSG, respectively. DMGs and DEGs were mapped on *B. mori* chromosomes, and we found that the density of m^{6}A modifications, different m^{6}A modifications, and gene density on chromosomes were highly consistent with each other. In most *B. mori* chromosomes, downregulated and upregulated DEGs were distributed uniformly. However, the downregulated DEGs were enriched significantly at the telomeres of chromosomes 27 (Fig. 4A). Moreover, 261 downregulated and 222 upregulated genes had upregulated m^{6}A modification levels. A total of 438 and 614 genes with downregulated m^{6}A modification levels were downregulated and upregulated, respectively. These results revealed that JHA widely regulates gene expression and mainly downregulates gene expression by regulating m^{6}A modification of mRNA. Notably, 2304 DEGs were not DMGs, and 1455 DMGs were not DEGs (Fig. 4B–C). Comparing m^{6}A peak lengths between the control and JHA treatment groups revealed that JHA treatment significantly decreased the length of mRNA, which was modified by m^{6}A (Fig. 4D). Through statistical analysis of the number of m^{6}A peaks in each gene, we found that most genes had one or two m^{6}A peaks. JHA treatment decreased the proportion of genes with one or two m^{6}A peaks and increased the number of genes with three m^{6}A peaks (Fig. 4E). These results show that JH affects the density and distribution of m^{6}A modifications, thereby regulating m^{6}A-containing gene expression.

Enrichment analysis of differentially m^{6}A-modified DEGs after JHA treatment

To investigate the effects of JHA treatment on silkworm PSGs, we performed GO and KEGG enrichment analyses of genes with different expression levels and m^{6}A peaks in RNA-seq and m^{6}A-seq data. We found DEGs with significantly different m^{6}A modifications after JHA treatment. To uncover the function of these genes, we performed GO enrichment analysis. Most of the genes were enriched in molecular function terms related to binding activity, especially nucleic acid binding activity. Two cellular component terms, nucleus and protein-containing complex, as well as five biological process terms, gene expression and biological regulation, were enriched in the GO analysis (Fig. S3). The results further confirmed that m^{6}A modification affected the fate of nucleic acids by regulating nucleic acid binding and nuclear components, thereby regulating gene expression and biological processes. KEGG enrichment analysis of these 547 genes found that 8 pathways, including autophagy, Hippo signaling pathway, MAPK signaling pathway, mTOR signaling pathway, nucleocytoplasmic transport, protein processing in endoplasmic reticulum, spliceosome, and Wnt signaling pathway, were highly enriched (Fig. 5). In total, 61 of 72 DEGs in these 8 pathways were downregulated after JHA treatment. All DEGs were downregulated in 4 pathways, including the Hippo signaling pathway, nucleocytoplasmic transport, spliceosome, and protein processing in the endoplasmic reticulum. The results suggested JHA affects multiple biological processes in PSGs through m^{6}A modification.

JHA treatment regulated the m^{6}A modification and expression level of silk-associated genes

To better understand the effect of JHA on silk protein synthesis in PSGs, we conducted an analysis of the expression changes in silk-associated genes, which are critical for silk protein synthesis, transport, and silk fiber formation (Table S1) [31]. These silk-associated genes were grouped into three functional categories: protease inhibitors, silk proteins, and transcription factors. Among these silk-associated genes, 32 genes were identified in transcriptome sequencing data (Fig. 6A), and 16 genes were significantly differentially expressed (Fig.S4). We further performed qPCR of 6 silk-associated genes to identify the reliability of RNA-sequencing. The result of qPCR confirmed the transcriptome data (Fig.S5). In addition, 6 of the 35 silk-associated genes showed significant changes in m^{6}A modification (Fig. 6B–F), suggesting that these genes are targets of m^{6}A modification. Notably, m^{6}A modification was mainly concentrated in the 3' UTRs and CDS regions of these 6 silk-associated genes. Furthermore, we observed that JHA resulted in different m^{6}A modification changes for different gene transcripts. JHA significantly increased the m^{6}A modification levels of *seroin 1*, *proteasome inhibitor PI31*, and *BmSPI4*. However, the m^{6}A modification levels of *sericin 2*, *BmSPI5*, and *Ldb* were downregulated by JHA. Taken together, the results suggest that the expression of *BmSPI4*, *BmSPI5*, *sericin2*, and *seroin1* is regulated by m^{6}A modification.

Knocking down *METTL3* regulated the expression level of silk-associated genes

To investigate the role of m^{6}A in the expression of silk-associated genes, we further knocked down the expression of *METTL3* in embryonic of silkworm. Through transcriptome sequencing data analysis, we identified 3561 DEGs after *METTL3* knockdown, and 1359 DEGs were

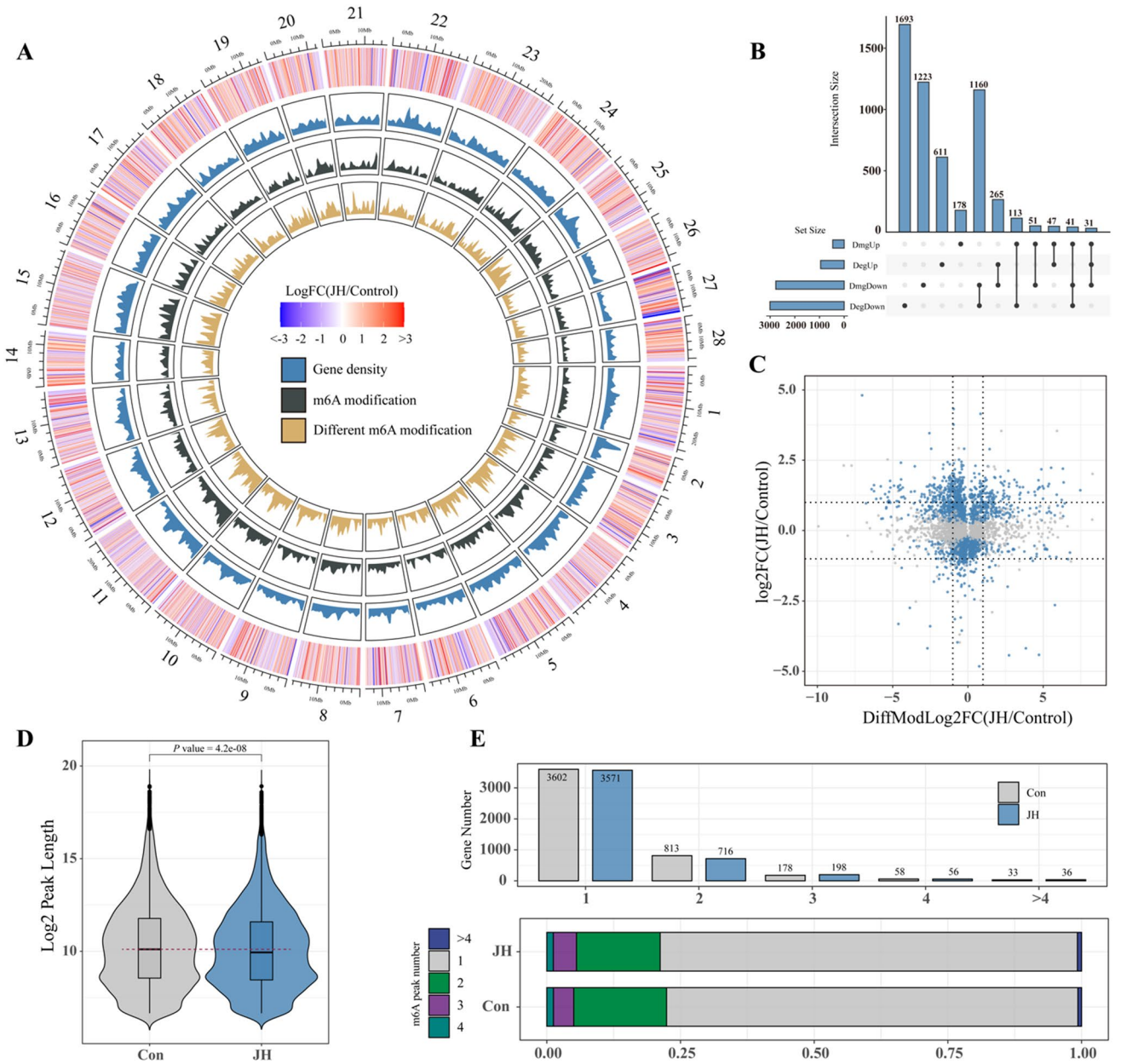

Fig. 4 JHA regulates m^{6}A modification of mRNA and gene expression in the silkworm PSG. Circos plot of the log2FC of DEGs, gene density, m^{6}A modification density, and DMGs on *B. mori* chromosomes, from the outside to the inside (**A**). Upset plot displayed the DEGs and DMGs identified in RNA-seq and m^{6}A-seq data (**B**). In the volcano plot, genes with significantly increased and decreased expression levels are highlighted in blue. The dashed line indicates y/x = ± 1 (**C**). Comparison of peak lengths of m^{6}A in silkworm PSGs in the control and JHA treatment groups (**D**). The number and proportion of genes with different m^{6}A peaks in the control and JHA treatment groups. The proportion of genes with 1, 2, 3, 4, and over 4 m^{6}A peaks were mapped in different color respectively (**E**)

m^{6}A-containing genes. The m^{6}A sequencing data in this study revealed that multiple genes in the JH signaling pathway are also m^{6}A-methylated (Table S2). Knocking down *METTL3* widely affected the expression of many genes in the JH signaling pathway, including *Juvenile hormone esterase 1* (*JHE1*), *Juvenile hormone epoxide hydrolase 2* (*JHEH2*), *Juvenile hormone epoxide hydrolase 3* (*JHEH3*), *Farnesyl pyrophosphate syntase* (*FPS*), etc. (Table S3). We further identified 32 silk-associated genes in the RNA-seq of silkworm embryos (Fig. 7A). In total, 11 silk-associated genes were DEGs (Fig. 7B). Interestingly, 5 DEGs, including *BmSPI4*, *BmSPI5*, *sericin2*, *Ldb*, and *seroin1*, had significantly different m^{6}A modification levels after JHA treatment in the PSG (Table S4). Taken together, the results

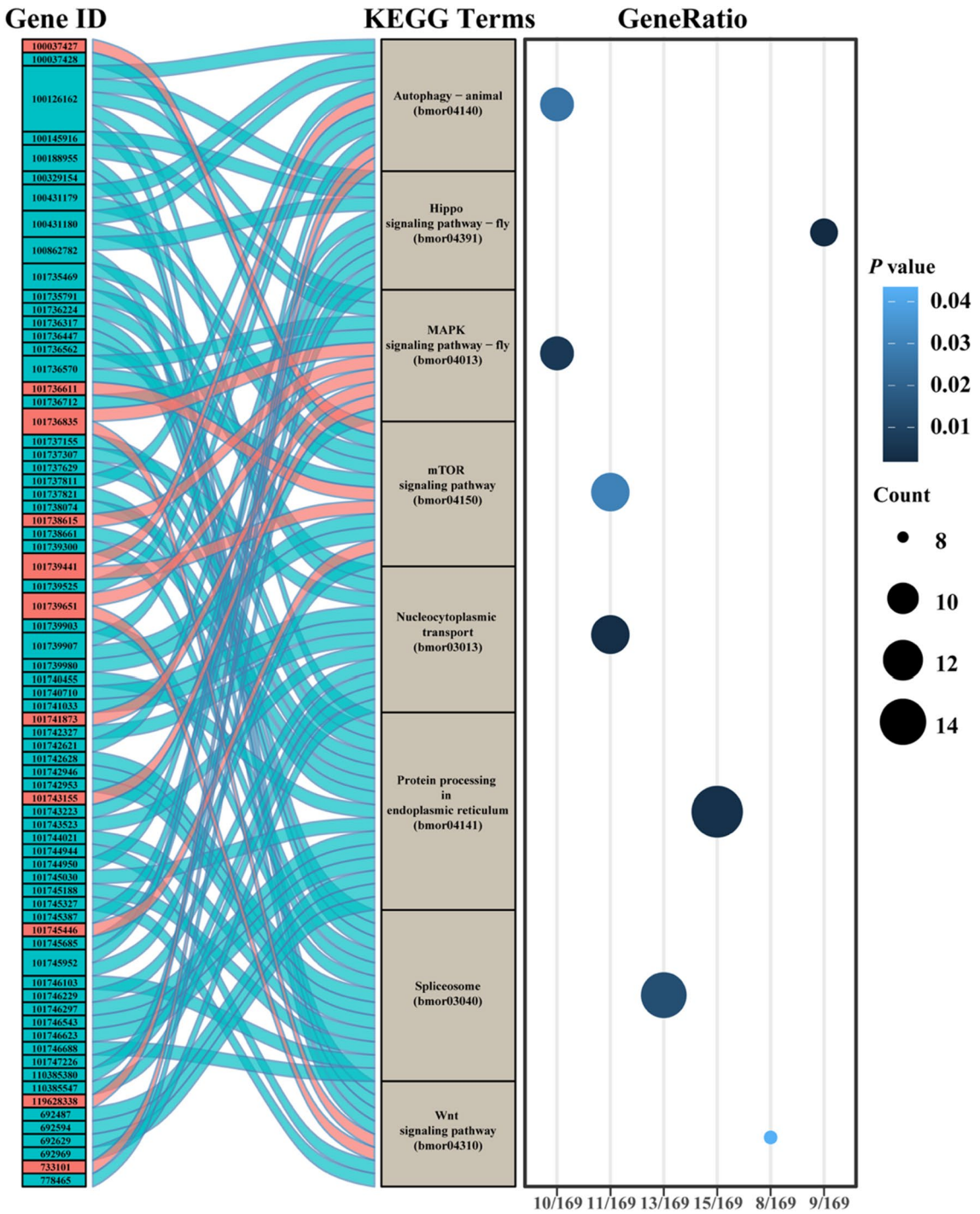

Fig. 5 KEGG enrichment analysis of genes with differential m^6A peaks and expression levels in silkworm PSG m^6A-seq data after JHA treatment. Genes with different m^6A peaks and expression levels were analyzed for KEGG enrichment. Eight KEGG terms with the highest gene counts were mapped. Seventy-two genes involved in these 8 KEGG terms are listed on the left-hand side of the Sankey plot. Blue and red blocks represent down- and up-regulated genes, respectively. The dot plot on the right-hand side of the analysis shows the gene counts, gene ratio, and *P* value of 8 KEGG terms

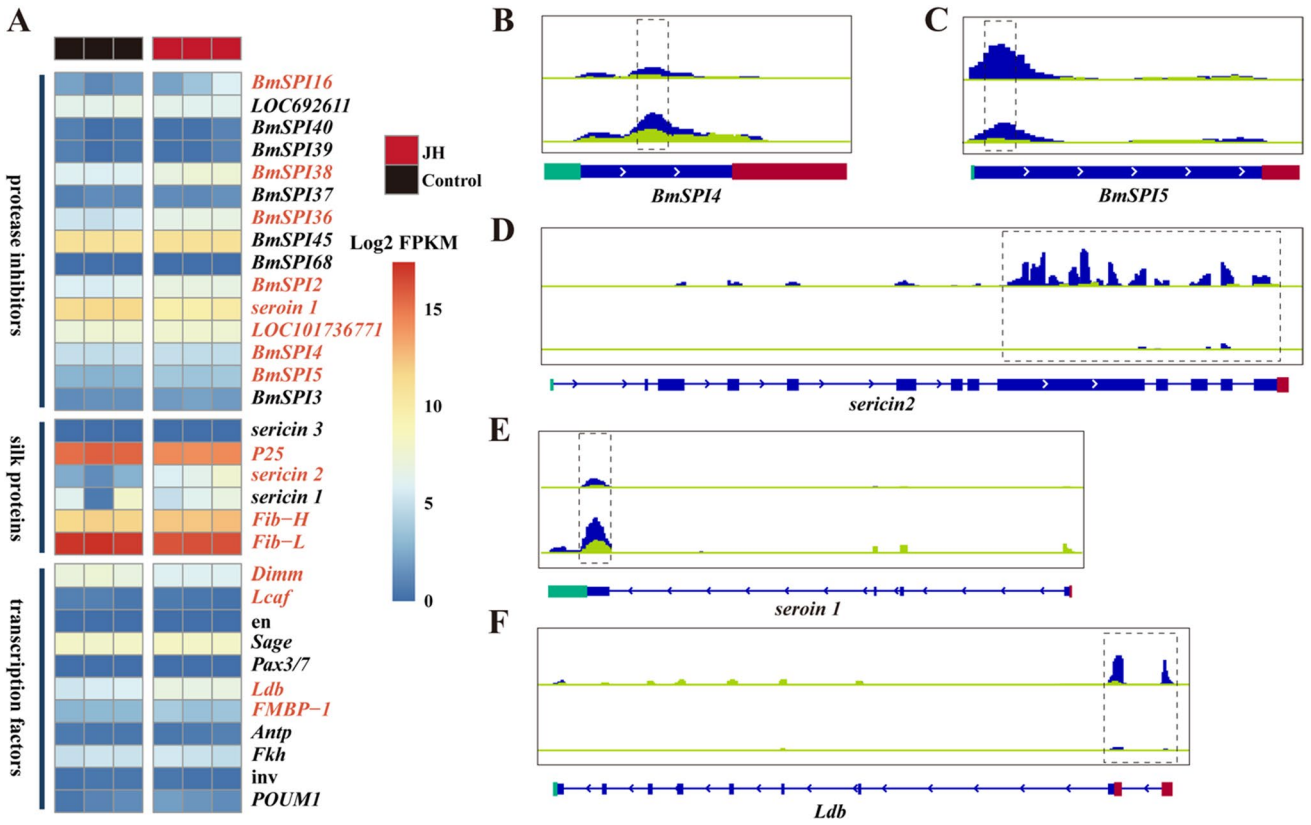

Fig. 6 Analysis of silk-associated genes in control and JHA-treated groups using RNA-seq and m^{6}A-seq data. Heatmap representing the Log2 FPKM of 32 silk-associated genes in RNA-seq data. Significantly regulated genes (P value < 0.05) were represented in red color (**A**). Silk-associated genes were grouped by their function in silk gland biological activities. IGV tracks in the blue panels display m^{6}A-seq reads, while the light green panels display RNA-seq reads, for 5 silk-associated genes along the locus in both control and JH-treated groups (**B**–**F**)

suggested that the expression of *BmSPI4*, *BmSPI5*, *sericin2*, and *seroin1* is regulated by m^{6}A modification.

JHA regulated the expression of *BmSPI4* and *BmSPI5* via m^{6}A modification

To investigate whether JH directly regulates silk-associated genes, we treated BmN cells with JHA for 2 h, 4 h, 6 h, 8 h, 12 h, and 24 h (Fig. 8A, Fig S6). The qPCR results suggested that JHA significantly increased the expression of *METTL3* and *YTHDF3* (Fig. 8A), and the results were confirmed by western blotting analysis (Fig. 8B). We also found that *BmSPI4* and *BmSPI5* were induced by JHA in BmN cells at 12 h. Given that JHA altered the m^{6}A modification levels of *BmSPI4* and *BmSPI5*, we therefore investigated whether JHA directly regulates the expression of *BmSPI4* and *BmSPI5* through m^{6}A in BmN cells. According to the results of m^{6}A sequencing, we identified that m^{6}A peaks in the *BmSPI4* CDS region ranged from NC_051385.1: 8,549,783–8,550,004, and the *BmSPI5* CDS region ranged from NC_051385.1: 8,506,603–8,506,712 (Fig. 8C). We further generated reporter plasmids containing His-tag following the wild-type *BmSPI4*, *BmSPI5*, or mutant *BmSPI4*, *BmSPI5* CDS. To avoid the influence of background expression of *BmSPI4* and *BmSPI5* in BmN cells, we designed specific qPCR primers located in the pIZ/V5-His vector, and *BmSPI4* or *BmSPI5* CDS regions (Fig. 8D). We performed qPCR and western blotting assays to detect the expression of PizV5-*BmSPI4* and PizV5-*BmSPI5* with or without JHA treatment. The results suggested that JHA treatment significantly enhanced the expression levels of pIZ/V5-*BmSPI4*-WT and PizV5-*BmSPI5*-WT (Fig. 8E–F). However, JHA did not improve the expression of pIZ/V5-*BmSPI4*-Mut or pIZ/V5-*BmSPI5*-Mut (Fig. 8E–F). Taken together, the results reveal that JHA directly regulates *BmSPI4* and *BmSPI5* through m^{6}A modification of CDS regions.

Discussion

In this study, we identified that JHA enhanced the weight and thickness of silkworm cocoons. Through conjoint analysis of RNA-seq and m^{6}A-seq, we uncovered the regulatory

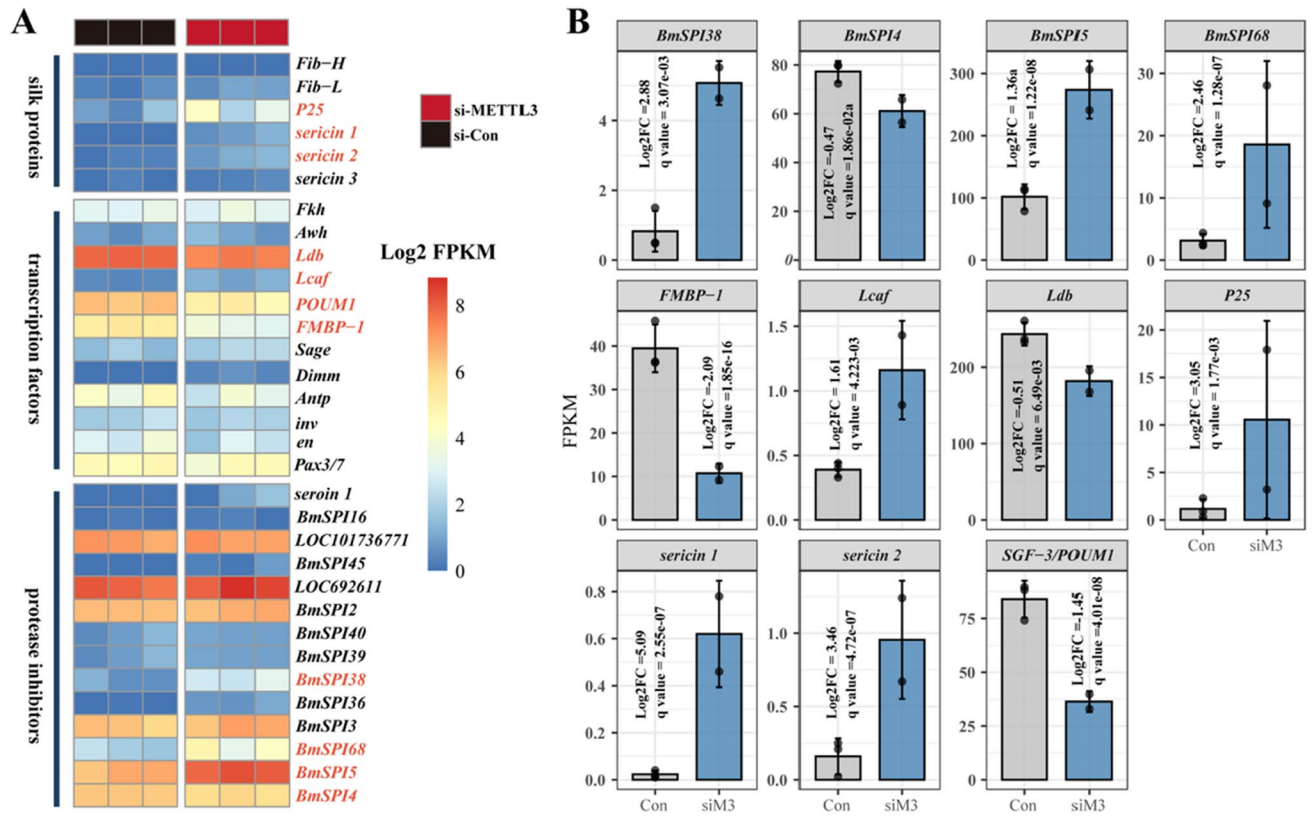

Fig. 7 Analysis of silk-associated genes in silkworm embryos of the control and siMETTL3 group using RNA-seq data. Heatmap representing the Log2 FPKM of 32 silk-associated genes in RNA-seq data after knocking down *METTL3* in the embryonic stage of silkworm. Significantly regulated genes (P value < 0.05) were represented in red color (**A**). Silk-associated genes were grouped by their function in silk gland biological activity. Bar charts representing 11 silk-associated genes that have significantly different expression in transcriptome data after knocking down *METTL3* (**B**)

relationship of JH to silk-associated gene expression levels by changing m^{6}A modification in silkworm PSG. Knockdown of *METTL3* further validated that many silk genes are targets of m^{6}A modification. Furthermore, we confirmed that JHA directly regulated expression of *BmSPI4* and *BmSPI5* through m^{6}A modification of the CDS regions in BmN cells. This study provided evidence in vivo and in vitro illustrating that m^{6}A modification plays a novel epigenetic mechanism in mediating the effects of JH. Our findings advance the understanding of the epitranscriptomic regulation of JH and provide new insights into the role of m^{6}A modification in insects.

Recent studies have focused on the relationship between JH and epigenetic modification [14]. Epigenetic modifications, acetylation and deacetylation, play critical roles in JH action. However, the correlation between JH and m^{6}A, the most prevalent chemical modification of eukaryotic RNA, is still unclear. An increasing number of studies have suggested that m^{6}A modification participates in numerous biological functions in mammals and insects [24, 25, 32]. In this study, we found that JHA treatment significantly induced the protein expression of METTL3 and YTHDF3 in silkworm PSG. We further performed m^{6}A methylation sequencing to characterize the profile of m^{6}A modifications in silkworm PSG. m^{6}A peaks are enriched in the CDS, especially around the stop codon region. The results showed that the m^{6}A distribution is conserved compared to that in other species [33, 34]. We also found m^{6}A peaks enriched in the start codon in silkworm PSG. Surprisingly, the peak in the start codon region did not appear in the mRNA of silkworm midgut and BmN cells [26, 27], suggesting that the feature of the m^{6}A modification in different tissues of silkworm has tiny differences. Further investigation is needed to fully understand the mechanism by which JHA regulates the expression of *METTL3* and *YTHDF3*.

m^{6}A modification has been shown to play a critical role in RNA-mediated regulation of numerous biological processes. In esophageal squamous cell carcinoma, m^{6}A modification regulates Notch1 expression and further promotes the activation of the Notch signaling pathway [35]. In this study, 16 m^{6}A-containing genes involved in the Notch signaling pathway were also enriched. In gastric cancer research, m^{6}A suppression enhanced GC cell proliferation and invasiveness by activating the Wnt signaling pathway [36]. The

Wnt signaling pathway was enriched after knocking down *METTL3* in the embryonic stage of silkworm [23]. Here, 40 m^{6}A-containing genes involved in the Wnt signaling pathway were also found in silkworm PSG. Collectively, these results showed that the correlation between m^{6}A and the Notch and Wnt signaling pathways might be conserved and widespread in eukaryotes. Knocking down *METTL3* also affected the expression of many genes in the JH signaling pathway including *JHE1*, *JHEH2*, *JHEH3*, *FPS*, *Hmg-r*, *Mk*, *Mpk*, etc. Compared to a study of *A. mellifera* [29], the m^{6}A sequencing data in this study revealed that multiple genes in the JH signaling pathway are also m^{6}A-methylated. Further experiments are required to determine the specific mechanisms by which METTL3 regulates the expression of many genes in the JH signaling pathway.

Silk secretion is one of the most mysterious and desirable biological phenomena in nature and has been studied for a long time, especially in *B. mori* and *Nephila clavipes* [37]. Transcriptome analysis of the *B. mori* silk gland, including the PSG and middle silk gland (MSG), showed that the PSG and MSG differ greatly in energy metabolism, silk protein synthesis and secretion [31]. Insect hormones are the critical factor controlling silk protein biosynthesis [38]. JH plays a crucial role in regulating silk gland development and silk fiber production in silkworm [3, 39, 40]. Moreover, previous reports highlighted that a JHA called methoprene could increase silk yield in silkworm [41, 42]. Here, we found that m^{6}A-related genes are regulated by JHA in the PSG.

Silk-associated genes are divided into three parts according to the function in the process of silk fiber formation. BmSPI4, BmSPI5, BmSPI36, BmSPI38, seroin2, etc. are protease inhibitors which are critical for protecting the silk protein from degrading by protease. Fib-L, Fib-H, seroin2, etc. are the components of silk fiber. Ldb, Dimm, sage etc. are important transcription factors for regulating the process of silk production. Here, we found that 16 silk-associated genes enriched in the PSG of silkworms had significantly different expression after JHA treatment. In this study, we further investigated the role of m^{6}A in mediating the effect of JH on PSG, especially in silk-associated genes. Five silk-associated genes, *BmSPI4*, *BmSPI5*, *seroin2*, *sericin2*, and *Ldb* were differentially m^{6}A methylated after JHA treatment. The results indicated that these genes are potential targets of m^{6}A modification. In the mammal animals, the m^{6}A reader protein YTHDF1 and YTHDF2 play essential roles in enhancing mRNA translation and degradation, respectively. So far we did not find YTHDF1 and YTHDF2 in the silkworm. In addition, the function of YTHDF3 in *B. mori* is still unclear. Further research about the mechanism of YTHDF3 regulating expression of silk-associated genes via recognizing m^{6}A modification is needed. In another aspect, silk-associated genes undergo regulating by complex system which is not limited in m^{6}A system [2, 3]. This also interpreted why the expression level of some genes is consistent with the m^{6}A modification level, while the other part is opposite.

To further identify the targets of m^{6}A, we altered the m^{6}A abundance by knocking down *METTL3*. METTL3, as the most important component of the m^{6}A transmethylase complex, plays a critical role in RNA m^{6}A modification [43]. Here, we found that knocking down *METTL3* led to changes in the expression level of many silk-associated genes. In addition, the results also suggested that the alternation of m^{6}A modification in different tendencies led to inverse expression changes in silk-associated genes. The results suggest that there is a direct regulatory mechanism of m^{6}A and silk-associated genes. Point mutagenesis of m^{6}A sites in the regions of the *BmSPI4* and *BmSPI5* CDSs further identified that m^{6}A plays a key role in enhancing the expression of *BmSPI4* and *BmSPI5* after JHA treatment. These results reveal that m^{6}A modification regulated by JH plays a significant role in regulating the expression of silk-associated genes in silkworm PSGs.

Concluding remarks

In summary, we characterized the detailed profile of m^{6}A modification in mRNA of silkworm PSG and revealed that many m^{6}A-related genes were regulated in the PSG of silkworm. m^{6}A marks in the PSG were differentially altered by JHA. Transcriptome and m^{6}A sequencing data show that JHA regulates numerous biological processes of PSG through m^{6}A modification. In addition, the data suggest that JHA regulates the expression of many silk associated genes in the PSG by m^{6}A methylation. Furthermore, we explored the mechanism by which JHA regulates the expression of silk associated genes through m^{6}A modification by knocking down *METTL3* and point mutant genesis. These results reveal the essential role of m^{6}A methylation regulated by JH in silk gland development and silk production. These results may help to overcome sericultural bottleneck. More importantly, this study demonstrates that m^{6}A modification is a critical factor mediating the effect of JH in insects.

Experimental procedures

Methylated RNA immunoprecipitation and sequencing

Total RNA of silkworm larvae PSG at the 3rd day of the 5th instar was isolated with TRIzol. Poly RNA was purified from 50 μg of total RNA using Dynabeads Oligo 25–61,005. The poly RNA was fragmented into small pieces using the

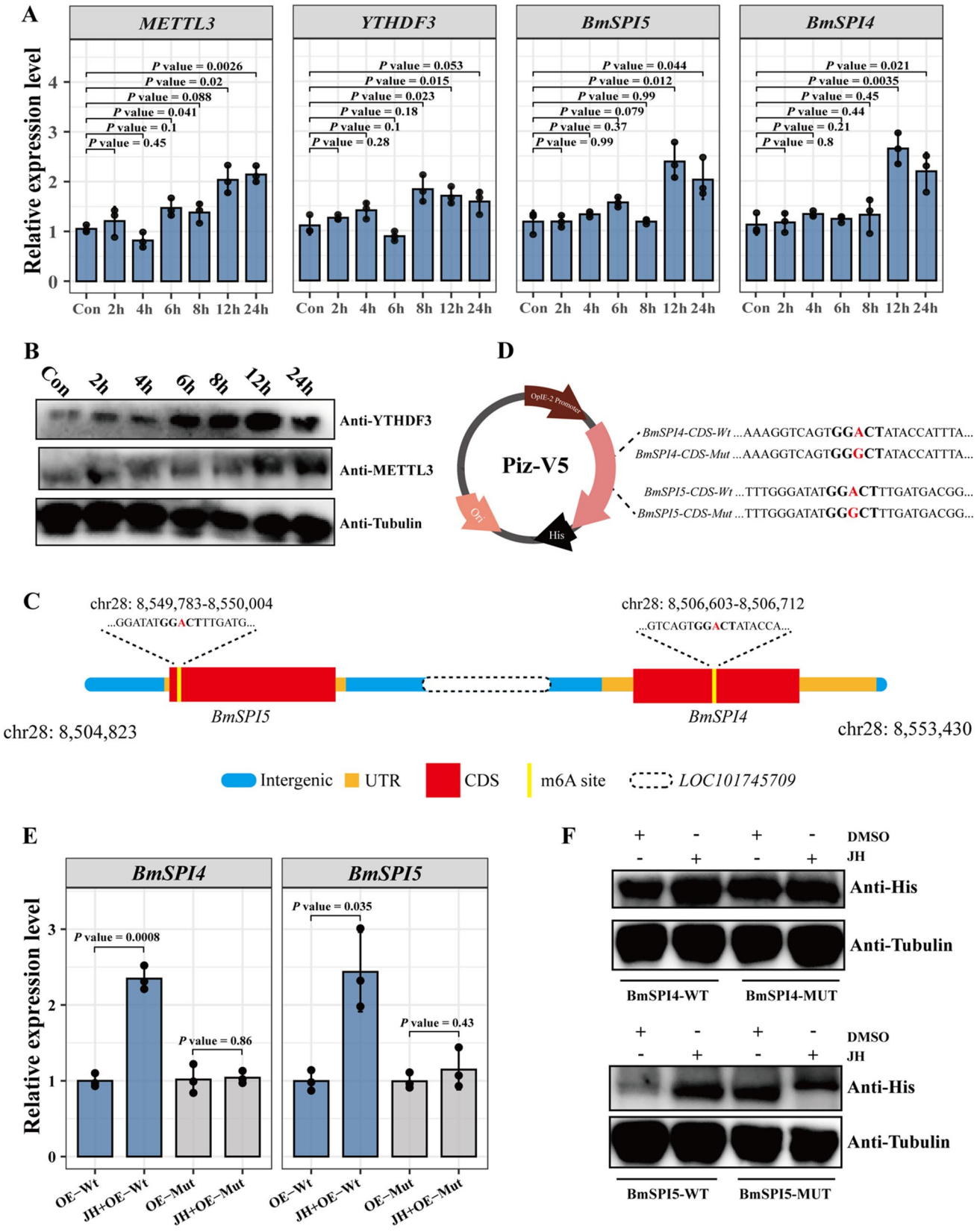
A
METTL3
YTHDF3
BmSPI5
BmSPI4
Relative expression level
P value = 0.0026
P value = 0.02
P value = 0.088
P value = 0.041
P value = 0.1
P value = 0.45
P value = 0.053
P value = 0.015
P value = 0.023
P value = 0.18
P value = 0.1
P value = 0.28
P value = 0.044
P value = 0.012
P value = 0.99
P value = 0.079
P value = 0.37
P value = 0.99
P value = 0.021
P value = 0.0035
P value = 0.45
P value = 0.44
P value = 0.21
P value = 0.8
Con 2h 4h 6h 8h 12h 24h
B
Con 2h 4h 6h 8h 12h 24h
Anti-YTHDF3
Anti-METTL3
Anti-Tubulin
D
Piz-V5
OpIE-2 Promoter
Ori
His
BmSPI4-CDS-Wt ...AAAGGTCAGTGGACTATACCATTTA...
BmSPI4-CDS-Mut ...AAAGGTCAGTGGGCTATACCATTTA...
BmSPI5-CDS-Wt ...TTTGGGATATGGACTTTGATGACGG...
BmSPI5-CDS-Mut ...TTTGGGATATGGGCTTTGATGACGG...
C
chr28: 8,549,783-8,550,004
...GGATATGGACTTTGATG...
chr28: 8,506,603-8,506,712
...GTCAGTGGACTATACCA...
BmSPI5
BmSPI4
chr28: 8,504,823
chr28: 8,553,430
Intergenic
UTR
CDS
m6A site
LOC101745709
E
BmSPI4
BmSPI5
Relative expression level
P value = 0.0008
P value = 0.86
P value = 0.035
P value = 0.43
OE−Wt
JH+OE−Wt
OE−Mut
JH+OE−Mut
F
DMSO
JH
Anti-His
Anti-Tubulin
BmSPI4-WT
BmSPI4-MUT
BmSPI5-WT
BmSPI5-MUT

◂**Fig. 8** Expression of *BmSPI4* and *BmSPI5* was directly regulated by JHA through m^{6}A modification in BmN cells. qPCR results of *METTL3*, *YTHDF3*, *BmSPI4*, and *BmSPI5* after JHA treatment for 2 h, 4 h, 6 h, 8 h, 12 h, and 24 h in BmN cells (**A**). Protein expression of METTL3 and YTHDF3 in BmN cells after JHA treatment for 2 h, 4 h, 6 h, 8 h, 12 h, 24 h, and 24 h was measured by western blotting analysis (**B**). Schematic representation of the positions of m^{6}A motifs within *BmSPI4* and *BmSPI5*. The elements of genes were presented in different color. Intergenic region, UTR, CDS and m^{6}A sites were mapped in blue, brown, red and yellow, respectively (**C**). Schematic representation of mutated CDS regions of *BmSPI4* and *BmSPI5*, which were cloned into the pIZ/V5 vector (**D**). qPCR and western blotting of pIZ/V5-BmSPI4-WT, pIZ/V5-BmSPI4-Mut, pIZ/V5-BmSPI5-WT, and pIZ/V5-BmSPI5-Mut in the control and JHA treatment groups (**E** and **F**)

Magnesium RNA Fragmentation Module and then incubated with m^{6}A-specific antibody in IP buffer at 4 °C for 2 h. After reverse transcription of the IP RNA to cDNA using SuperScript™ II Reverse Transcriptase, the cDNA was used to synthesize U-labeled second-stranded DNA with *E. coli* DNA polymerase I, RNase H and dUTP Solution. Following ligation with indexed adapters, size selection was performed with AMPureXP beads. After U-labeled second-stranded DNA was treated with the heat-labile UDG enzyme, the ligated products were amplified by PCR. Finally, paired-end sequencing on an Illumina Novaseq™ 6000 platform was performed according to the vendor's recommended protocol.

Sequencing data analysis

Trim-galore was used to remove the reads that contained adaptor contamination, low-quality bases and undetermined bases with default parameters. FastQC was used to verify the sequence quality of the IP and input samples. STAR was used to map reads to the reference genome of *B. mori*. The peaks were called and analyzed using MACS2 and subsequently annotated using the ChIPseeker R package. After peak calling of m^{6}A peaks with MACS2, the bed file with the sites and annotation of m^{6}A peaks on *B. mori* genome was imported in R, and further made the Txdb object which having the information of starting and ending of transcripts with R package Guitar. And then, the density of m^{6}A peaks on transcripts was calculated and plotted with the function GuitarPlot from R package Guitar. De novo and known motif finding were performed using the MEME suite and HOMER. RSEM was used to perform expression level estimation for all transcripts and genes from input libraries by calculating FPKM. Furthermore, DEGs were identified using the edgeR R package with thresholds of $|\log2FC| \geq 1$ and p value < 0.05. GO and KEGG enrichment analyses of genes were performed using the ClusterProfiler R package. The data are presented as the mean ± SD from at least three repeated biological and technical experiments. The p value was calculated using two-tailed unpaired Student's t test between two groups in R with a p value < 0.05 considered statistically significant.

Measurement of cocoon parameters

The cocoons were cut open carefully, and the pupae were separated before calculating the shell weight and cocoon thickness. The shell weight was measured in grams with an electronic digital balance. The thickness of each cocoon shell was measured in millimeters using a fabric thickness meter with a presser foot area of 50 mm^2 and pressure of 0.2 ± 0.0005 kPa.

Sample preparation

The domesticated silkworm strain (Qiufeng × Baiyu) was reared in 25 °C incubator with fresh mulberry. For juvenile hormone (JH), juvenile hormone analog (JHA) (Yuanye Bio-Technology, China) was used instead of JH in larvae. Acetone was used for dissolving and applying JHA. The tissues of silkworm were collected and extracted for total RNA after JHA treating 24 h at L5D3.

Cell culture, treatments, and transfection

BmN cells were maintained in Sf-900 II SFM medium (Thermo Fisher Scientific, USA) with 3% fetal bovine serum (Gibco, USA). JHA and DMSO in final concentration 3 μM was used to treat BmN cells for 2 h, 4 h, 6 h, 8 h, 12 h, and 24 h. For overexpression of *BmSPI4*, *BmSPI5I*, BmN cells were transfected with plasmids by Lipo8000 (Beyotime, China) according to the manufacturers' instructions. After transfected with pIZ/V5-BmSPI4-CDS-WT, pIZ/V5-BmSPI4-CDS-Mut, pIZ/V5-BmSPI5-CDS-WT or pIZ/V5-BmSPI5-CDS-Mut for 24 h, BmN cells were further treated with or without JHA (3 μM) for 12 h.

RNA extraction and qPCR

RNA isolation and reverse transcription-quantitative PCR were performed as described before [23]. Briefly, total RNA extracted from *B. mori* tissues and BmN cells using Trizol Plus (TaKaRa, Japan) were used for cDNA synthesis. All the primers used in qPCR assays were list in Table S4 and the amplification efficiencies of the qPCR primers were between 90 and 110% ($R^2 > 0.98$). qPCR assays were performed using SYBR green detection method. Gene expression was analyzed using three biological replicates and three technical replicates and normalized to the control gene *BmRpl49*.

Western blotting analysis

Western blot analysis was conducted as described in our previous study [23]. Briefly, silkworm PSG and BmN cells were collected and washed with pre-cool phosphate-buffered saline (PBS) as well as mechanically homogenized in ice-cold RIPA (FDbio Science, China) lysate (RIPA: PMSF = 100: 1) for 30 min. The protein content of the supernatant was quantified using bicinchoninic acid (BCA) assay. Equal quality of protein (15 μg) was separated by SDS-PAGE, and then transferred into PVDF membranes (Millipore, USA). The membranes were blocked with no-fat milk and treated overnight with polyclonal rabbit/mouse anti-METTL3, anti-YTHDF3, anti-Tubulin, or anti-His. After incubated with a secondary antibody (DingGuo ChangSheng Biotechnology, China) for 2 h, the ECL Plus Kit (FDbio Science, China) were used to detected signal.

Construction of plasmids for overexpression of *BmSPI4* and *BmSPI5*, and purification of recombinant YTHDF3 (1-152aa)

The ORFs encoding the *BmSPI4* and *BmSPI5* were cloned into pIZ/V5-His vector respectively. 1–456 bp of *YTHDF3* CDS was cloned into pCold-His vector (TaKaRa, Japan). All the primers were listed in Table S4.

Protein purification of recombinant YTHDF3 (1-152aa) and preparation of antiserum

YTHDF3 CDS (1-456bp) was subcloned into Pcold-His vector (TaKaRa, Japan) with 6 × His-tag at the C-terminus, and then transfected to *Escheerichia coli* (BL21, Tsingke, China). *E. coli* was raised in Luria–Bertani medium at 37˚C for 6 h and 18˚C for 18 h. The *E. coli* was collected and dissolved with ice-cold lysis solution and sonication for 30 min. The supernatant was collected after centrifuged for 30 min at 13,000 rpm and 4 °C, and purified with Ni-nitrilotriacetic acid (NTA) column (GE Healthcare, USA) as described in our previous study[23]. Western blotting and CBB staining were used to identify the purity of recombinant YTHDF3 (1-152aa) (Fig. S6). Purified protein was used to generate rabbit polyclonal antibody according to previous study [44].

Detection of m^{6}A abundance in total RNA

m^{6}A modification of total RNA was determined in four duplicates using the EpiQuick RNA Methylation Quantification Kit. Two hundred nanograms of total RNA was utilized per assay well and incubated with binding solutions at 37 °C for 90 min. After washing three times, capture antibody was added to each assay well, incubated for 60 min at room temperature and washed. Then, detection antibody was added and incubated at room temperature for 30 min. After washing three times with washing buffer, the enhancer solution for 30 min and the determined solution for 10 min away from the light were used. The signal was detected at 530/590 nm after the addition of fluorescence developer using a MultiSkan FC microplate reader.

Supplementary Information The online version contains supplementary material available at https://doi.org/10.1007/s00018-023-04996-1.

Acknowledgements We thank Yinghui Li and Jianguo Tao for directions and assistance of cocoon thickness and weight measurement. We also thank Shiyu Zou and Zhihua Hao for silkworm rearing and tissues dissection.

Author contributions S.L., H.T., and H.W. conceived the study, and designed the experiments. S.L., H.T., and H.W. performed experiments and most data analyses. Y.X., and H.W. contributed reagents or analytical tools. S.L., and H.W. wrote the manuscript draft. All authors read and approved the final manuscript.

Funding This work was supported by the Natural Science Foundation of Zhejiang Province (Grant No. LR22C040001), the National Natural Science Foundation of China (Grant No. 319704603; 32170483), the Zhejiang Provincial Science and Technology Plans (2021C02072-6), and the Zhejiang Provincial Key Laboratory Construction Plans (2020E10025).

Availability of data and material All data are available in the manuscript and in the Supplementary Information. m^{6}A sequencing and transcriptome sequencing data of JHA treatment in silkworm PSG have been uploaded in the National Center for Biotechnology Information Sequence Read Archive with accession number: PRJNA948114. The RNA-seq of knocking down *METTL3* in the embryonic of silkworm in our previous study were also uploaded with accession number: PRJNA882243. All the codes generated in the study have been uploaded in Github (https://github.com/Shuaiqi-Liu/JH-m6A).

Declarations

Conflict of interest The authors declare no conflict of interest with the contents of this article.

Ethical approval and consent to participate Not applicable.

Consent for publication All authors read and approved the final manuscript.

References

1. Jindra M, Palli SR, Riddiford LM (2013) The juvenile hormone signaling pathway in insect development. Annu Rev Entomol 58:181–204. https://doi.org/10.1146/annurev-ento-120811-153700
2. Zhao X-M, Liu C, Jiang L-J, Li Q-Y, Zhou M-T, Cheng T-C et al (2015) A juvenile hormone transcription factor Bmdimm-fibroin H chain pathway is involved in the synthesis of silk protein in silkworm, *Bombyx mori*. J Biol Chem 290:972–986. https://doi.org/10.1074/jbc.M114.606921

3. Li G, Lan H, Lu Q, He C, Wei Y, Mo D et al (2021) The JH-Met2-Kr-h1 pathway is involved in pyriproxyfen-induced defects of metamorphosis and silk protein synthesis in silkworms, *Bombys mori*. Pesticide Biochem Physiol 179:104980. https://doi.org/10.1016/j.pestbp.2021.104980
4. Cao J, Zheng H, Zhang R, Xu Y, Pan H, Li S et al (2023) Dimmed gene knockout shortens larval growth and reduces silk yield in the silkworm, *Bombys mori*. Insect Mol Biol 32:26–35. https://doi.org/10.1111/imb.12810
5. Wang J-L, Zhang Y-P, Gu Y-Y, Wang J-X, Zhao X-F (2009) Function of a TGF-β inducible nuclear protein in the silk gland in *Bombyx mori*. Insect Mol Biol 18:243–251. https://doi.org/10.1111/j.1365-2583.2008.00861.x
6. Liu L, Wang Y, Li Y, Ding C, Zhao P, Xia Q et al (2019) Crosstalk between juvenile hormone and ecdysone regulates transcription of fibroin modulator binding protein-1 in *Bombyx mori*. Int J Biol Macromol 128:28–39. https://doi.org/10.1016/j.ijbiomac.2019.01.092
7. Brindha S, Maragathavalli S, Gangwar SK, Annadurai B (2012) Effect of Juvenile hormone on enhance silk production in *Bombyx mori*. IJABR 2:396–402
8. Bownes M, Dübendorfer A, Smith T (1984) Ecdysteroids in adult males and females of *Drosophila melanogaster*. J Insect Physiol 30:823–830. https://doi.org/10.1016/0022-1910(84)90019-2
9. Gilbert LI, Rybczynski R, Warren JT (2002) Control and biochemical nature of the ecdysteroidogenic pathway. Annu Rev Entomol 47:883–916. https://doi.org/10.1146/annurev.ento.47.091201.145302
10. Kozlova T, Thummel CS (2000) Steroid regulation of postembryonic development and reproduction in *Drosophila*. Trends Endocrinol Metab 11:276–280. https://doi.org/10.1016/S1043-2760(00)00282-4
11. Truman JW, Riddiford LM (2002) Endocrine insights into the evolution of metamorphosis in insects. Annu Rev Entomol 47:467–500. https://doi.org/10.1146/annurev.ento.47.091201.145230
12. Minakuchi C, Zhou X, Riddiford LM (2008) Krüppel homolog 1 (Kr-h1) mediates juvenile hormone action during metamorphosis of *Drosophila melanogaster*. Mech Dev 125:91–105. https://doi.org/10.1016/j.mod.2007.10.002
13. Pray-Grant MG, Grant PA (2020) Ant-icipating change: an epigenetic switch in reprogramming the social lives of ants. Mol Cell 77:205–206. https://doi.org/10.1016/j.molcel.2019.12.006
14. Roy A, Palli SR (2018) Epigenetic modifications acetylation and deacetylation play important roles in juvenile hormone action. BMC Genom. https://doi.org/10.1186/s12864-018-5323-4
15. Xu J, Roy A, Palli SR (2018) CREB-binding protein plays key roles in juvenile hormone action in the red flour beetle, *Triboloum Castaneum*. Sci Rep 8:14–26. https://doi.org/10.1038/s41598-018-19667-6
16. Wang X, Zhao BS, Roundtree IA, Lu Z, Han D, Ma H et al (2015) N6-methyladenosine modulates messenger RNA translation efficiency. Cell 161:1388–1399. https://doi.org/10.1016/j.cell.2015.05.014
17. Holoch D, Moazed D (2015) RNA-mediated epigenetic regulation of gene expression. Nat Rev Genet 16:71–84. https://doi.org/10.1038/nrg3863
18. Chandola U, Das R, Panda B (2015) Role of the N6-methyladenosine RNA mark in gene regulation and its implications on development and disease. Brief Funct Genom 14:169–179. https://doi.org/10.1093/bfgp/elu039
19. Alarcón CR, Lee H, Goodarzi H, Halberg N, Tavazoie SF (2015) N6-methyladenosine marks primary microRNAs for processing. Nature 5:482–519. https://doi.org/10.1038/nature14281
20. Alarcón CR, Goodarzi H, Lee H, Liu X, Tavazoie S, Tavazoie SF (2015) HNRNPA2B1 is a mediator of m^{6}A-dependent nuclear RNA processing events. Cell 162:299–308. https://doi.org/10.1016/j.cell.2015.08.011
21. Frye M, Harada BT, Behm M, He C (2018) RNA modifications modulate gene expression during development. Science 361:1346–1349. https://doi.org/10.1126/science.aau1646
22. Yang Y, Hsu PJ, Chen Y-S, Yang Y-G (2018) Dynamic transcriptomic m^{6}A decoration: writers, erasers, readers and functions in RNA metabolism. Cell Res 28:616–624. https://doi.org/10.1038/s41422-018-0040-8
23. Liu S, Jia S, Tian H, Li Y, Hu K, Tao J et al (2023) Evolution of m^{6}A-related genes in insects and the function of *METTL3* in silkworm embryonic development. Insect Mol Biol 32:316–327. https://doi.org/10.1111/imb.12832
24. Kan L, Ott S, Joseph B, Park ES, Dai W, Kleiner RE et al (2021) A neural m^{6}A/Ythdf pathway is required for learning and memory in *Drosophila*. Nat Commun 12:1458. https://doi.org/10.1038/s41467-021-21537-1
25. Haussmann IU, Bodi Z, Sanchez-Moran E, Mongan NP, Archer N, Fray RG et al (2016) m^{6}A potentiates Sxl alternative pre-mRNA splicing for robust *Drosophila* sex determination. Nature 540:301–304. https://doi.org/10.1038/nature20577
26. Yang X, Wei X, Yang J, Du T, Yin C, Fu B et al (2021) Epitranscriptomic regulation of insecticide resistance. Sci Adv. https://doi.org/10.1126/sciadv.abe5903
27. Zhang X, Zhang Y, Dai K, Liang Z, Zhu M, Pan J et al (2020) N6-methyladenosine level in silkworm midgut/ovary cell line is associated with *Bombyx mori* nucleopolyhedrovirus infection. Front Microbiol 10:2988. https://doi.org/10.3389/fmicb.2019.02988
28. Li B, Wang X, Li Z, Lu C, Zhang Q, Chang L et al (2019) Transcriptome-wide analysis of N6-methyladenosine uncovers its regulatory role in gene expression in the lepidopteran *Bombyx mori*. Insect Mol Biol 28:703–715. https://doi.org/10.1111/imb.12584
29. Wang M, Xiao Y, Li Y, Wang X, Qi S, Wang Y et al (2021) RNA m^{6}A modification functions in larval development and caste differentiation in honeybee (*Apis mellifera*). Cell Rep 34:108–580. https://doi.org/10.1016/j.celrep.2020.108580
30. Roundtree IA, Evans ME, Pan T, He C (2017) Dynamic RNA modifications in gene expression regulation. Cell 169:187–200. https://doi.org/10.1016/j.cell.2017.05.045
31. Shi R, Ma S, He T, Peng J, Zhang T, Chen X et al (2019) Deep insight into the transcriptome of the single silk gland of *Bombyx mori*. IJMS 20:2491. https://doi.org/10.3390/ijms20102491
32. Liang Y, Han H, Xiong Q, Yang C, Wang L, Ma J et al (2021) METTL3-mediated m^{6}A methylation regulates muscle stem cells and muscle regeneration by Notch signaling pathway. Stem Cells Int. https://doi.org/10.1155/2021/9955691
33. Meyer KD, Saletore Y, Zumbo P, Elemento O, Mason CE, Jaffrey SR (2012) Comprehensive analysis of mRNA methylation reveals enrichment in 3′ UTRs and near stop codons. Cell 149:1635–1646. https://doi.org/10.1016/j.cell.2012.05.003
34. Lence T, Akhtar J, Bayer M, Schmid K, Spindler L, Ho CH et al (2016) m^{6}A modulates neuronal functions and sex determination in *Drosophila*. Nature 540:242–247. https://doi.org/10.1038/nature20568
35. Han H, Yang C, Zhang S, Cheng M, Guo S, Zhu Y et al (2021) METTL3-mediated m^{6}A mRNA modification promotes esophageal cancer initiation and progression via Notch signaling pathway. Mol Ther Nucleic Acids 26:33–46. https://doi.org/10.1016/j.omtn.2021.07.007
36. Zhang C, Zhang M, Ge S, Huang W, Lin X, Gao J et al (2019) Reduced m^{6}A modification predicts malignant phenotypes and augmented Wnt/PI3K-Akt signaling in gastric cancer. Cancer Med 8:4766–4781. https://doi.org/10.1002/cam4.2360

37. Sutherland TD, Young JH, Weisman S, Hayashi CY, Merritt DJ (2010) Insect silk: one name, many materials. Annu Rev Entomol 55:171–188. https://doi.org/10.1146/annurev-ento-112408-085401
38. Maekawa H, Suzuki Y (1980) Repeated turn-off and turn-on of fibroin gene transcription during silk gland development of *Bombyx mori*. Dev Biol 78:394–406. https://doi.org/10.1016/0012-1606(80)90343-7
39. Hirayama C, Nakamura M (2002) Regulation of glutamine metabolism during the development of *Bombyx mori* larvae. Biochimica et Biophysica Acta (BBA) 1571:131–137. https://doi.org/10.1016/S0304-4165(02)00207-6
40. Daillie J (1979) Juvenile hormone modifies larvae and silk gland development in *Bombyx mori*. Biochimie 61:275–281. https://doi.org/10.1016/S0300-9084(79)80072-3
41. Miranda JE, de Bortoli SA, Takahashi R (2002) Development and silk production by silkworm larvae after topical application of methoprene. Sci Agric (Piracicaba, Braz) 59:585–588. https://doi.org/10.1590/S0103-90162002000300026
42. Chaitanya RK, Sridevi P, Senthilkumaran B, Dutta GA (2013) Effect of juvenile hormone analog, methoprene on H-fibroin regulation during the last instar larval development of Corcyra cephalonica. Gen Comp Endocrinol 181:10–17. https://doi.org/10.1016/j.ygcen.2012.08.014
43. Liu J, Yue Y, Han D, Wang X, Fu Y, Zhang L et al (2014) A METTL3–METTL14 complex mediates mammalian nuclear RNA N6-adenosine methylation. Nat Chem Biol 10:93–95. https://doi.org/10.1038/nchembio.1432
44. Lee B-S, Huang J-S, Jayathilaka LP, Lee J, Gupta S (2016) Antibody production with synthetic peptides. In: Schwartzbach SD, Skalli O, Schikorski T, (Eds). High-resolution imaging of cellular proteins. Springer, New York. pp. 25–47. https://doi.org/10.1007/978-1-4939-6352-2_2.